# Humanlike Inverse Kinematics for Improved Spatial Awareness in Construction Robot Teleoperation: Design and Experiment

Tianyu Zhou, Ph.D., S.M.ASCE[1]; Qi Zhu, Ph.D., Aff.M.ASCE[2]; Yang Ye, S.M.ASCE[3]; and Jing Du, Ph.D., M.ASCE[4]

**Abstract:** The teleoperation of robotic arms is expected to play a key role in dangerous or inaccessible construction workplaces. Most robot arms rely on mechanical designs that are completely different from human arms. It could lead to a risk that certain joints move with undesired poses and cause collisions because of the mismatch between robot mechanical design and human operators' egocentric perception of their own arms. This paper proposes an innovative robotic control method that mimics the human shoulder-arm structure, enabling human operators to teleoperate with unfamiliar robotic arms intuitively. A two-tracker system is used to map human arm motions into a revised robotic inverse kinematics (IK) algorithm called humanlike IK. One tracker controls the end effector of the robot, and the other tracker drives the middle joint of the robot, analogous to how a human moves the arm. A seven-degree-of-freedom robotic arm was repurposed based on the revised IK. A human-subject experiment ($n = 26$) was performed to test the effectiveness of the proposed humanlike IK method in a pipe maintenance task. Results confirmed the performance and functional benefits of the proposed method. It can inspire the design of a new robot teleoperation method for dexterous tasks in construction. **DOI: 10.1061/JCEMD4.COENG-13350.** 

**Author keywords:** Inverse kinematics (IK); Robotic arm; Pipe skid; Human factors.

## Introduction

Robot teleoperation, i.e., manipulating a robotic system from a distance, has been well explored by many industries to improve safety and performance in human-unfriendly tasks including hazardous materials handling (Qian et al. 2012), search and rescue (Cavallin and Svensson 2009), confined area inspection (Kim et al. 2019), and remote assembly and installation (Qin et al. 2016). It has been found that robot teleoperation leverages the advantages of human uncertainty in decision making and the physical capacities of robotic systems in dynamic and dangerous tasks (Hirche and Buss 2012; Yang et al. 2016). Specifically, the use of industrial manipulators, usually in the form of robotic arms, has demonstrated the potential to overcome complex tasks that require precise hand operations or dexterous operations, while also satisfying the human operator's desired actions and maintaining the robot's stability (Mathew et al. 2015; Siciliano and Khatib 2016; Stanton et al. 2012). Regarding dangerous and difficult construction activities, such as facility replacement and repair (R&R), teleoperating robotic arms enable humans as the commander for tasks challenged by complex procedures and dynamic environments (Hirche and Buss 2012; Osawa et al. 2017; Rakita et al. 2018; Zhou et al. 2020), rather than completely relying on robotic intelligence, which could be immature in the foreseeable future (Hitz et al. 2014).

Furthermore, future construction operations can happen in altered workplaces with distinct contexts, requiring complex dexterous coordination or relating to environments that are less accessible or unsafe for human workers, such as underwater construction, power plant turnaround maintenance, and offshore rig operations (Shou et al. 2018; Shukla and Karki 2016; Vu et al. 2019). As such, teleoperating robotic arms are considered more effective and safer for these future construction operations (Chen et al. 2007; Niemeyer et al. 2016; van Osch et al. 2014).

There are different ways for realizing the control of a remote robotic arm, such as through the use of hand props (e.g., joysticks), programmable inputs, and keyboards (Jiang et al. 2013; Thirumurugan et al. 2010). Among all, bilateral control is considered the most intuitive, which is critical to the scalable deployment of robot teleoperation. Bilateral control enables a human operator to control the movements of a distant robotic system via motion mirroring, for directing the movement of a remote robot arm by moving the control device in a similar manner (Anderson and Spong 1988). Recent human body motion-capture technologies have enabled human operators to use their own body components, particularly the hands, to guide the end effector (e.g., the tip of a robot arm) of the remote robot in a mirrored way (Zhou et al. 2020; Zhu et al. 2022).

[1]Informatics, Cobots, and Intelligent Construction (ICIC) Lab, Dept. of Civil and Coastal Engineering, Univ. of Florida, Gainesville, FL 32611. Email: zhoutianyu@ufl.edu

[2]Postdoctoral Research Associate, Informatics, Cobots, and Intelligent Construction (ICIC) Lab, Dept. of Civil and Coastal Engineering, Univ. of Florida, Gainesville, FL 32611. Email: qizhu@ufl.edu

[3]Ph.D. Student, Informatics, Cobots, and Intelligent Construction (ICIC) Lab, Dept. of Civil and Coastal Engineering, Univ. of Florida, Gainesville, FL 32611. Email: ye.yang@ufl.edu

[4]Associate Professor, Informatics, Cobots, and Intelligent Construction (ICIC) Lab, Dept. of Civil and Coastal Engineering, Univ. of Florida, Gainesville, FL 32611; Professor, Dept. of Mechanical and Aerospace Engineering, Univ. of Florida, Gainesville, FL 32611; Professor, Dept. of Industrial and System Engineering, Univ. of Florida, Gainesville, FL 32611 (corresponding author). ORCID: https://orcid.org/0000-0002-0481-4875. Email: eric.du@essie.ufl.edu

Note. This manuscript was submitted on November 16, 2022; approved on February 15, 2023; published online on April 22, 2023. Discussion period open until September 22, 2023; separate discussions must be submitted for individual papers. This paper is part of the ***Journal of Construction Engineering and Management***, © ASCE, ISSN 0733-9364.

The locations and poses of other robotic arm joints are then controlled using inverse kinematics (IK), which involves recovering the positions and rotations of each robot arm joint based on the intended movement trajectory of a single end effector (Aristidou et al. 2018).

However, because traditional IK focuses on the single-point estimate toward the end effector of the robot, it may result in unwanted and unanticipated movement of remaining joints, leading to possible collision problems in confined areas. Specifically, there are two potential problems with the traditional IK in practice. First, most IK algorithms rely on approximating the solution of a Jacobian matrix, and hence the solution is not unique (Aristidou et al. 2018). With that said, for the same end-effector trajectory, the recovered joint positions can be different at times. It is therefore difficult for human operators to predict the movements of robotic arm joints other than the end effector. For work in restricted places, if only the end effector of the remote robot follows human movements, the remaining joints may engage in unintended motions that are not expected by the human operator, inducing problems such as a collision between the robotic arm and the surrounding objects (Ikuta et al. 2003; Kanehiro et al. 2004).

Second, the robot arm's mechanical designs often differ from that of a human arm (e.g., additional joints); thus, it is challenging for the human operator to coordinate activities that may require far-reaching movements of the robotic arm in a safe manner, such as stretching the entire robotic arm to reach an object. This is particularly serious for robot arms with a large number of degrees of freedom (DOFs). For example, because most IK algorithms aim to minimize the movement distance (economic consideration), the middle joint of 7-DOF robotic arms (i.e., the elbow position) does not always follow the motion of the elbow of the human operator, resulting in an ungainly chicken wing posture that is rarely seen in humans (Reddivari et al. 2014). The difference between robotic arms and a human arm can impair the natural spatial awareness of the human operator in dexterous tasks, making the bilateral control in restricted areas more difficult.

This work presents a novel IK method for the teleoperation of robot arms that is humanlike. The so-called humanlike IK is a proposed algorithm that uses motion trackers on key joints of a human arm to track human motions in terms of the pose of the arms, adds additional IK inputs for more natural recovery of the robot arm elbow positions and rotations, and drives the robot arm to move in a more natural, humanlike manner. The interactive virtual reality (VR) system was developed based on our previous systems (Du et al. 2016, 2018a, b, 2017; Shi et al. 2018; Zhou et al. 2022; Zhu et al. 2021). The humanlike IK is also adapted to be compatible with the Robot Operating System (ROS) (Quigley et al. 2009). To quantify the effectiveness of humanlike IK versus the traditional IK methods, we performed a human-subject experiment using the Franka Emika Panda robot simulation. The remainder of the paper will introduce the relevant literature, the system design, and the findings of the human-subject experiment.

## Literature Review

### Human–Robot Interaction

Effective robot teleoperation relies on a carefully designed human–robot interaction (HRI). The concept of HRI is rooted in research in the area of manufacturing robotic platforms, which "extends a person's sensing and/or manipulating capabilities to a position remote from that person" (Sheridan 1992). Existing research, such as that by Yanco and Drury (2002), asserts that HRI is a subset of wider human–computer interaction (HCI) issues because robots are computer systems, whereas HCI is concerned with the design, assessment, and implementation of interactive computing systems. Nonetheless, it is important to emphasize that the concepts of teleoperated robot interface design diverge significantly from normal HCI lessons learned in these dimensions, including the physical specifications and morphologies of robots, the number of systems a user may be called to interact with simultaneously interaction roles; the dynamic nature of the robot platform, and the roles of interaction where human agents play (Scholtz 2003). According to this definition, teleoperation HRI is defined as the interaction between a single human and a single robot in which the person (operator) issues orders to one robot and the robot responds with sensor data (Yanco and Drury 2004). A sufficient amount of human consciousness is required to ensure a working HRI, particularly for teleoperation duties (Doisy et al. 2017). The human operator must be aware of the robot's environment and status, and the robots must respond to human directions in a natural manner (Drury et al. 2003).

However, maintaining accurate and up-to-date situational awareness is a challenging problem in construction tasks subject to changing and unpredictable environments that can potentially impair platform and perceptual capabilities (Murphy 2004). In addition, given the noncollocated condition, the lack of synchronized awareness can result in improper commands from the operator and unexpected executions by the robot. Recent advances in interfaces motivate the research for a new solution for developing trustworthy, safe, and efficient teleoperation control methods to achieve an enhanced HRI (Bonci et al. 2021). On the one hand, the development of sensor technologies significantly advances robot capabilities to perceive the environment and also to monitor human behavior, and plan appropriate robot responses in different phases of collaborative tasks (Ishida et al. 2018; Peternel et al. 2017). More modalities, including visual, aural, and haptic input, are used, on the other hand, to increase human situational awareness of what is going on throughout the collaborative job (Casalino et al. 2018). One of the ways that have been demonstrated to be beneficial for increased awareness of robot teleoperation is the bilateral control (Opiyo et al. 2021). Bilateral control leverages a master-subordinate architecture, where the operator controls the master system and the subordinate system mirrors the motion data from the master (Yokokohji and Yoshikawa 1994). Usually, the motion mirroring does not require the reproduction of the complete master system. IK is used to recover the motion dynamics of the subordinate system based on only incomplete data from the master system (Aristidou et al. 2018). The following section explains the IK methods for robotic arm control.

### Inverse Kinematics for Robotic Manipulator Controls

To move the end effector to the desired position, IK, or the use of kinematic equations to determine the joint parameters of a manipulator (Aristidou et al. 2018), is utilized. Numerous IK methods have been developed, such as the analytical method (Craig 2009), numerical method (Buss 2004), and artificial neural network (El-Sherbiny et al. 2018). The mathematic efficiency and reliability of IK have been well validated in the robotics (Sciavicco and Siciliano 2012) and computer science literature (Aristidou et al. 2018). Analytical approaches are designed to determine all feasible solutions based on the lengths of the mechanism, the starting posture, and the rotation constraints, and they are usually dependent on some assumptions (Aristidou et al. 2018).

Much robotic research uses analytical IK solutions to control end effectors, such as solving general 6R manipulators (Manocha and Canny 1994; Raghavan and Roth 1993) and multibody mechanisms (Gan et al. 2005; Paul and Shimano 1979). IKFast (Diankov 2010) is an analytical tool for solving robot IK equations and deploying motion planning algorithms in real-world robot applications. MoveIt! is a suite of software packages for mobile manipulation that includes motion planning and collision avoidance and is connected with ROS (Chitta et al. 2012). Based on IKFast, this popular MoveIt! plugin offers analytic solvers for robotic arms like Baxter, Franka Panda, and Universal Robots (Chitta 2016).

Analytical IK solutions are reliable and rarely experience singularity difficulties because they provide a global solution. However, the nonlinear nature and lack of scalability of kinematic equations make them unsuitable for redundant systems (Aristidou et al. 2018). The MoveIt! package is reliable for real robot control but it is time-consuming for digital twin (DT) simulation.

Cyclic coordinate descent inverse kinematics (CCDIK) (Luenberger and Ye 1984; Wang and Chen 1991) is an iterative heuristic technique for controlling an articulated body interactively. CCDIK has been implemented for a variety of robotic applications in humanlike manipulation (Lander and Content 1998). The viability for creating and controlling highly articulated characters of CCDIK has been examined by Kenwright (2012). CCDIK provides a numerically stable solution with linear-time complexity in the number of degrees of freedom, resulting in a minimal computational cost for each iteration (Welman 1993). However, due to the redundancy of the robot, the CCDIK algorithm may return different trajectories: because most robotic arms have more than six degrees of freedom, CCDIK allows an infinite number of different solutions to the inverse kinematics problem for the same target position (Canutescu and Dunbrack 2003).

Numerical methods require a set of iterations to achieve a satisfactory solution. Iterative techniques define the problem by minimizing a cost function (Aristidou et al. 2018). The Jacobian J is a matrix of partial derivatives of the entire chain system with respect to the angle parameters $\theta$. The IK issue can be approximated linearly using Jacobian solutions. An excellent review of the Jacobian methods has been given by (Buss 2004). Jacobian methods tackle the IK problem iteratively by modifying the configuration of a complete chain so that the end-effector position and orientation move closer to a target position and orientation at each stage.

Existing IK research, on the other hand, has focused on how to improve IK efficiency rather than how to better produce humanlike movements. Because most robot arms have different joint structures from those of human arms, if a human operator teleoperates the robot based on personal own motor experience, the two agents' actions may cause misunderstanding or collision. Most modern robots are controlled by a single-target IK solver like Panda IK solver, MoveIt!, IKFast, or CCDIK, which is based on the positioning information of the end effector. Instead of analytical solutions, these IK algorithms typically provide numerical responses by approximating the desired locations. This means that the recovered pose of the robot arm's other joints may differ from case to case at the same end-effector position. It makes the bilateral control of a remote robot arm more unpredictable from a human perspective.

## Humanlike IK for Construction Tasks

### *Robot Control Architecture*

The first step toward realizing humanlike robot teleoperation in confined construction workplaces is to enable a seamless motion data exchange between human operators and the remote robot. ROS and the Unity game engine were utilized to achieve robotic control and human motion data capturing and processing. The game engine was used because it is robust in the real-time rendering of motion data. In addition, the game engine provides a platform for developing the entire robot teleoperation system in VR, which offers immersive and intuitive working spaces for human operators (Freina and Ott 2015). The arm kinematic data of human operators can be captured, transferred, and processed in Unity and then streamed seamlessly to ROS to enable real-time robotic control. The Unity-ROS data synchronization infrastructure is realized based on previous works (Pu et al. 2021; Xia et al. 2022; Zhou et al. 2020). The Emika Panda robot (Emika 2022) was selected as a functional example to validate the proposed architecture. Fig. 1 shows the system architecture of the ROS-Unity data synchronization.

As illustrated in Fig. 1, the robot control system mainly consists of three functions: ROS-based robot control, digital twin reconstruction and rendering in the game engine, and human mechanics capturing and conversion. ROS is used to subscribe to the input commands and control the robot's motion based on the desired pose. ROS also publishes the current state of the robot as an output to establish two-way communication. The communication between Unity and ROS can be established by ROS#. ROS# is a collection of open-source software libraries in C#, which provides compatible application programming interfaces (APIs) to facilitate bidirectional communication between ROS and Unity (Siemens 2019). In the context of robot teleoperation, data transmission among distributed working stations is necessary. We utilized ROSbridge to provide a JSON data stream between ROS and Unity (Crick et al. 2017), which enables data transmission via a public network, such as the internet. ROSbridge provides a WebSocket server for Unity to interact with, serving as a connection between ROS and the network (Crick et al. 2017). The ROS server converts robotic dynamics data into JSON messages via ROSbridge and publishes it to or receives it from the internet, then converts it to ROS messages (Crick et al. 2017; Quigley et al. 2009), which are further utilized to control the robot.

On the Unity side, ROS# facilitates the construction of Unity nodes that are compatible to publish and receive data from ROS topics. ROS# establishes a WebSocket that subscribes to data from .NET applications (GitHub 2019) so that Unity can connect to a computer with a specified internet protocol (IP) address and exchange data through a network. We granted the ROS server and Unity's WebSocket the same IP address so that Unity and ROS can share data seamlessly: the ROS server publishes/subscribes to the processed ROS topics, and Unity subscribes to all ROS topics and publishes commands in specific ROS topics. The subscribed ROS topics stream robot state data to Unity and control the behavior of a digital robot arm replica in Unity. The digital replica, or digital twin of the robot arm, was built from a Unified Robot Description Format (URDF) file of the robot (Wiki 2019). The URDF digital twin model has the same digital configurations and parameters as the real robot arm such that it is compatible to receive data from subscribed ROS topics and behaves the same as the real robot. Unity can subscribe to the *joint_states* ROS topic, which includes the real-time location and orientation of each robot joint. The pose and state of the robot arm's digital twin then can be synchronized with the real robot arm.

For human operators, the robot's digital twin model and virtual pipe skid model are shown in the immersive virtual environment. When holding the VR controller in their hands and wearing the VR tracker on their elbow, human operators' arm poses can be tracked and processed as command inputs for the robot arm. Human operators can complete the tasks naturally utilizing their spatial awareness and collision-avoiding path planning strategy. The natural



J. Constr. Eng. Manage., 2023, 149(7): 04023044

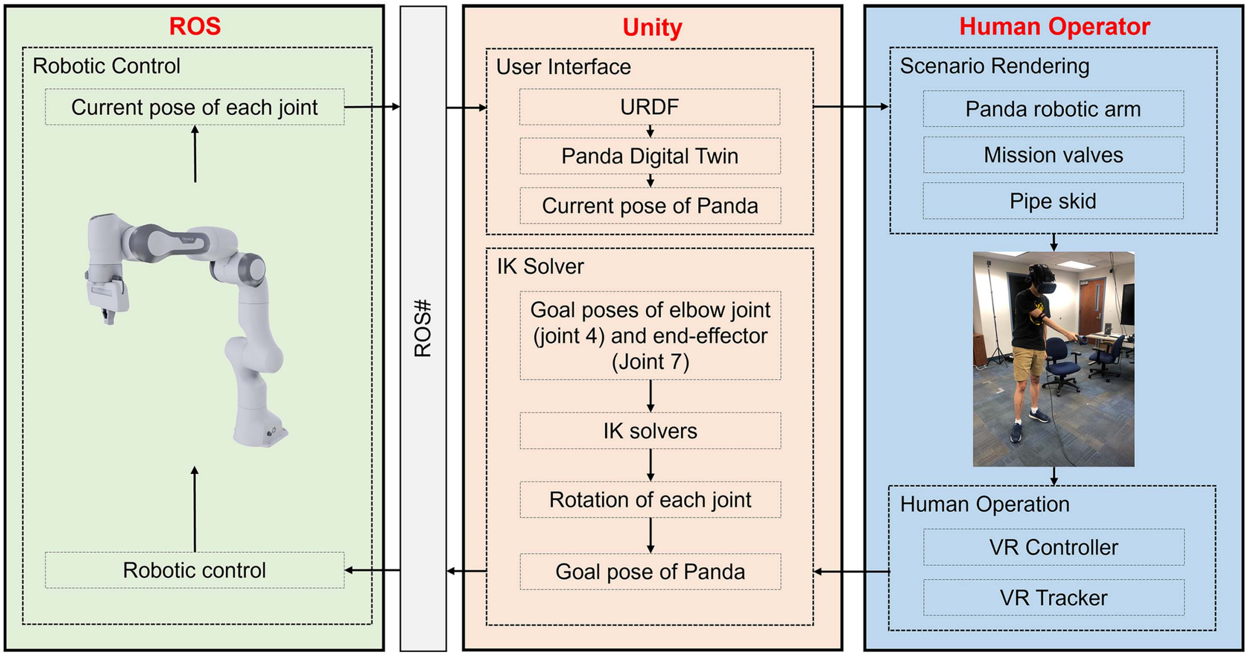


**Fig. 1.** System architecture of ROS-Unity data synchronization.

posture of human kinematics can be abstracted and transferred as two key points: hand posture and elbow posture, which are further used as robot end effectors and intermediate joint commands. The abstracted human kinematics are then transferred to Unity for further processing. An IK solver is utilized to recover the entire desired robot state from the poses of the start joint (base joint) and the abstracted human kinematics. The desired robot pose can be transmitted to ROS based on ROS# to control the behavior of the real robot. Furthermore, the converged real robot state will be subscribed by Unity to update the digital twin model of the robot arm and visualize it to users, which forms a closed loop.

### *Motion Tracking and Mapping*

The proposed system focuses on controlling the locomotion of robotic arms via human arm motions. The following stage is to design motion tracking on the human operator's arm and map the data to the corresponding joints of the robotic arm. Without loss of generality, we propose to generate humanlike robot arm motions by focusing on the robot elbow constraints. The literature has shown that the human elbow joint shares the biggest degree of freedom in upper-limb movements (Buckley et al. 1996). Reproduction of the human elbow joint's dynamics is critical to the cyclic voluntary movements (Bennett et al. 1992). As a result, numerous active systems, such as exoskeletons, focus on modeling the elbow joint movements (Lenzi et al. 2011; Li et al. 2020).

To capture precise human motion features as inputs to IK solvers, a retrofitted version of the HTC Vive headset (HTC Corporation, New Taipei City, Taiwan) (Tobii Pro VR Integration, Tobii Pro, Danderyd, Stockholm, Sweden), a VR controller, and a VR tracker, are used in this study. As illustrated in Fig. 2, the human operator needs to wear the HTC Vive headset on their head, hold the VR controller in their hand, and wear the VR tracker on their elbow.

The mapping between a human arm and the robotic arm depends on the design of the IK method. Specifically, instead of using one IK solver to control the robot arm based on the pose of the end effector directly, our proposed humanlike IK adds a pose constraint to the robot elbow joint based on the tracker attached to the human operator's elbow. Therefore, the robot arm is divided into two segments. The lower segment from the base to the middle joint of the robot corresponds to the upper arm of the human operator, whereas the upper segment from the middle joint to the end effector of the robot matches the forearm and hand of the human operator. However, different robots may have different selections of the intermediate joint. In this research, the 7-DOF Emika Panda robot was selected as the functional example.

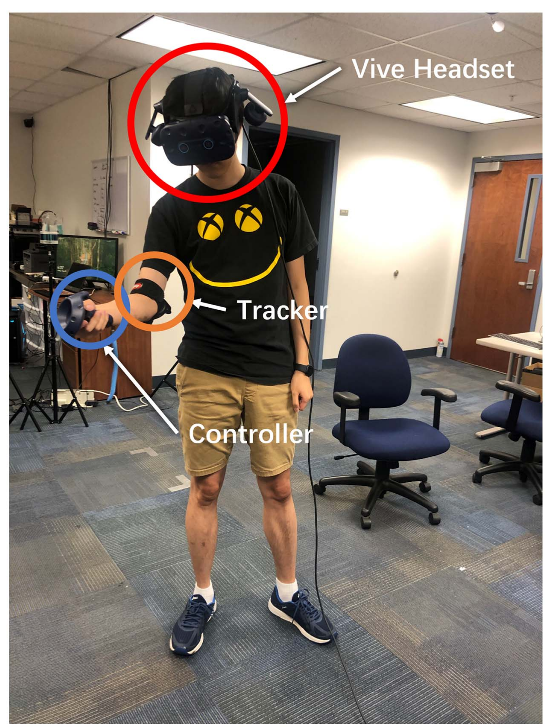


**Fig. 2.** Human operator wears the Vive headset, tracker, and controller.

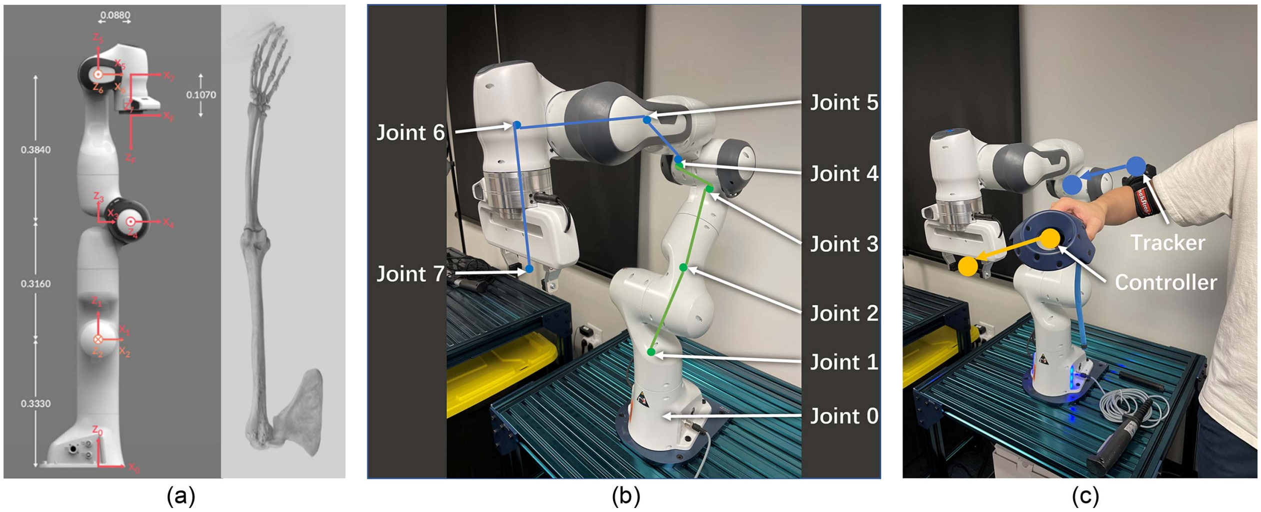


**Fig. 3.** Robot specification, human arm motion tracking, and mapping to the robotic arm.

As illustrated in Fig. 3(a), the locations and movement features of robot Joints 3, 4, and 5 are, respectively, similar to the shoulder yaw rotation, elbow pitch rotation, and wrist yaw rotation of the human arm joint, we selected Joint 4 as the intermediate joint for the proof of concept. Joint 4 is the middle part of the robot arm, which can be intuitively mapped to the human elbow, and the end effector is mapped to the human hand. This is sufficient for driving the motion of a robotic arm close to that of a human arm. Figs. 3(b and c) illustrate how human arm motions were tracked and mapped onto corresponding joints of the Emika Panda robotic arm.

Additionally, we configured a robot start mechanism for remote operation. The trigger button on the VR controller was configured to activate and deactivate the robotic arm. The operator can use the button to initiate the end effector of the robotic arm to follow the controller's trajectory or to stop the robot and maintain its posture. The start mechanism can only be activated if the distance between the controller and the end effector is less than 20 cm. The purpose of this mechanism is to prevent errors caused by the operator pressing the button while the controller was still distant from Panda's arm. This could prevent Panda's arms from moving too quickly in an undesirable direction, resulting in collisions. During the experiment, the human operators were allowed to change the operating location. When the operators want to observe the situation of the workspace, they can inactivate the control of the robot, walk around to have a better understanding of the state of the robot, and go to a suitable location to continually activate and control the robot.

### Revised IK Solver

As mentioned previously, the humanlike IK divides the robot arm into two segments. We used two IK solvers to obtain the positions of the joints, respectively. As illustrated in Fig. 3(a), using the Emika Panda robot as the example, the arm was divided into Joints 0–4 and Joints 4–7. Each part was regarded as a robot arm with four DOFs. The IK solvers of two segments of the robot arm were built based on the Jacobian solutions in Unity. Because the IK solvers with four DOFs may not yield a stable result, we set a tolerance of 5° for each joint. The desired pose of each IK solver was defined by the VR tracker and VR controller, as shown in Fig. 3(b). The VR tracker on the operator's elbow provided the desired pose of Joint 4, and the controller on the operator's hand provided the desired position of Joint 7. Because the pose of Joint 1 is fixed, IK solvers can rely on the target poses of Joints 4 and 7 to find the rotation of each joint.

We used the Jacobian Moore-Penrose pseudoinverse (Penrose 1955) algorithm to calculate the IK. The Appendix illustrates the details of the Newton-Raphson IK method used in this study. For the traditional IK with only inputs from the end effector, the angle vector is

$$\{\Theta\} = \{\theta_1, \theta_2, \theta_3, \theta_4, \theta_5, \theta_6, \theta_7\}^T \tag{1}$$

In contrast, the proposed humanlike IK considers two vectors of the two IK solvers

$$\{\Theta'\} = \{\theta_1, \theta_2, \theta_3, \theta_4\}^T \quad \text{and} \quad \{\Theta''\} = \{\theta_4, \theta_5, \theta_6, \theta_7\}^T \tag{2}$$

The robot can be remotely controlled to complete the task based on the desired rotation of each joint.

## Human-Subject Experiment

### Overview

To further test the effectiveness of the proposed humanlike IK method in construction robot teleoperation, we performed a human-subject experiment based on the proposed system. We selected a pipe skid facility R&R task as the test case. The objective of this task was to control the industrial robot to trigger the target valve while avoiding collisions. The pipe skid was chosen because of its high appearance in particularly confined workspaces. We modeled a 7-DOF Emika Panda robot mounted on a base for maintenance tasks and recorded the occurrence of all three-dimensional (3D) regions containing collisions in an immersive virtual environment, as shown in Fig. 4.

To evaluate the control algorithm, unwanted collision events between the robot and the pipe needed to be recorded. We recognized and agreed that the control mechanism, once established, would require validation of real-world data before it could be deployed in real-world circumstances. However, a collision between a real robot and a real pipe can be hazardous and potentially cause robot damage. Therefore, the immersive virtual robot and pipe were built to replicate the real-world interaction. To ensure two robots have identical poses, we utilized URDF to construct a virtual robot and

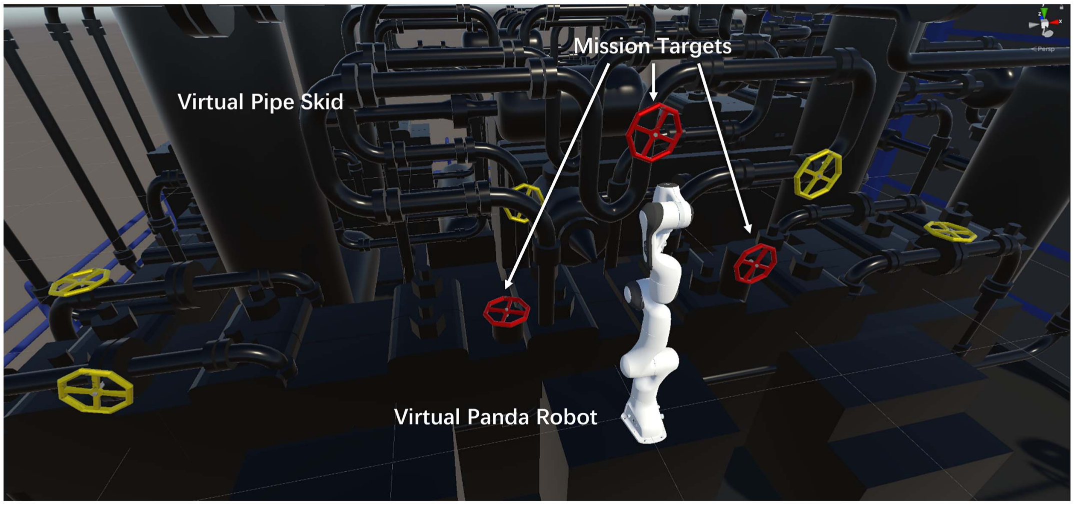


**Fig. 4.** Pipe skid and robot for the human-subject experiment.

transferred the *joint_states* data to VR. The VR environment was designed to elicit similar behavioral responses to those observed in real-world work contexts, and so was suitable for pipe skid maintenance tasks. Given the ease of data collection and experiment manipulation, the use of VR for human behavioral data gathering has gained favor in the cognitive and behavioral literature (Kinateder et al. 2014).

### Data Collection System

For data collection, we used an interactive VR system with motion-tracking functions to collect participants' behavior data. A virtual working scenario of maintenance of a pipe skid in a confined space was designed as the task. In the experiment, participants were asked to control the robot to trigger three valves. The pipe skid was within the operating range for the robot's end effector to manipulate three rotary valves. Once the system detected a collision between the robot's end effector and the valve, this valve was tagged as triggered, and the mission status was recorded as complete. When all valves were triggered (i.e., the task is complete), the system automatically stopped data recording and ended the task trial.

To achieve the motion tracking and documentation functions in the VR, several C# scripts were developed based on Tobii Pro Software Development Kit (SDK) version 1.11.0 and the API in Unity. The system collected data on participants' hand movement, elbow movement, robot joint movement, task complete states, and collision times at a frequency of 90 Hz. After each VR experiment, the developed VR system automatically recorded the raw data and streamed it into a CSV file.

### Experiment Setting

To investigate the influence of embodiment control on task performance, two control algorithms were developed: (1) the traditional IK solver, i.e., the robot was controlled based on the target pose of the end effector, defined as the control condition; and (2) the proposed humanlike IK solver, i.e., the target poses of end effector and elbow joint were used to control the robot, defined as the test condition. As a control condition, we evaluated the control of the Panda robot based only on the traditional IK with input from the controller. As illustrated in Figs. 5(a–c), the pose of the Panda's end effector can be controlled to reach each valve. However, Joint 5 of the Panda robot is close to the pipe and prone to collisions when performing pipe maintenance. We also tested the Panda control based on the humanlike IK with inputs from the controller and the tracker as the test condition. As illustrated in Figs. 5(d–f), the operator could control the end effector to complete the tasks while keeping Joint 5 away from the pipe skid to prevent a collision. This could be because the humanlike IK could assist the human operator in controlling Panda's arms in a more humanlike manner, hence preventing collisions in this cramped work environment.

The other variables are the same between the two conditions. Participants' operation time, motion velocity, and collision times were collected during the experiment. In addition, we used a background questionnaire to collect participants' demographic information, and we applied three questionnaires [National Aeronautics and Space Administration (NASA) task load index (TLX) questionnaire (Hart and Staveland 1988), Situational Awareness Rating Technique (SART) survey (Taylor 2017), and Trust Scale questionnaire (Merritt 2011)] at the end of the experiment to evaluate participants' cognitive load, situational awareness, and trust level to validate the results.

The experiment consisted of five sessions: (1) training; (2) operation task under Condition 1; (3) questionnaires about Condition 1; (4) operation task under Condition 2; and (5) questionnaires about Condition 2. The training session, Session 1, was designed to familiarize participants with the robotic control mechanism and interactions within the virtual environment. Each participant was instructed to be acquainted with the VR devices (VR headset, VR controller, and VR tracker) and the virtual environment. Then, participants were given instructions about how to manipulate the robot arm to interact with the virtual valves based on two control algorithms. Participants were also instructed to avoid collisions as much as possible.

After the training session, participants were asked to perform the pipe maintenance task based on one control algorithm in the VR environment (Session 2). Because the task of the pipe maintenance was simple (triggering three valves), the participants were asked to perform the task 10 times for each condition to get more solid data because the repetition of the task could effectively reduce the impact of random error. In Session 3, after completing the operation session, participants were given questionnaires (NASA TLX, SART, and Trust Scale) to provide comments and feedback. Then, in Session 4, the participants were asked to perform the task based on another robot control algorithm and provide feedback based on questionnaires (Session 5). In order to eliminate the influence of

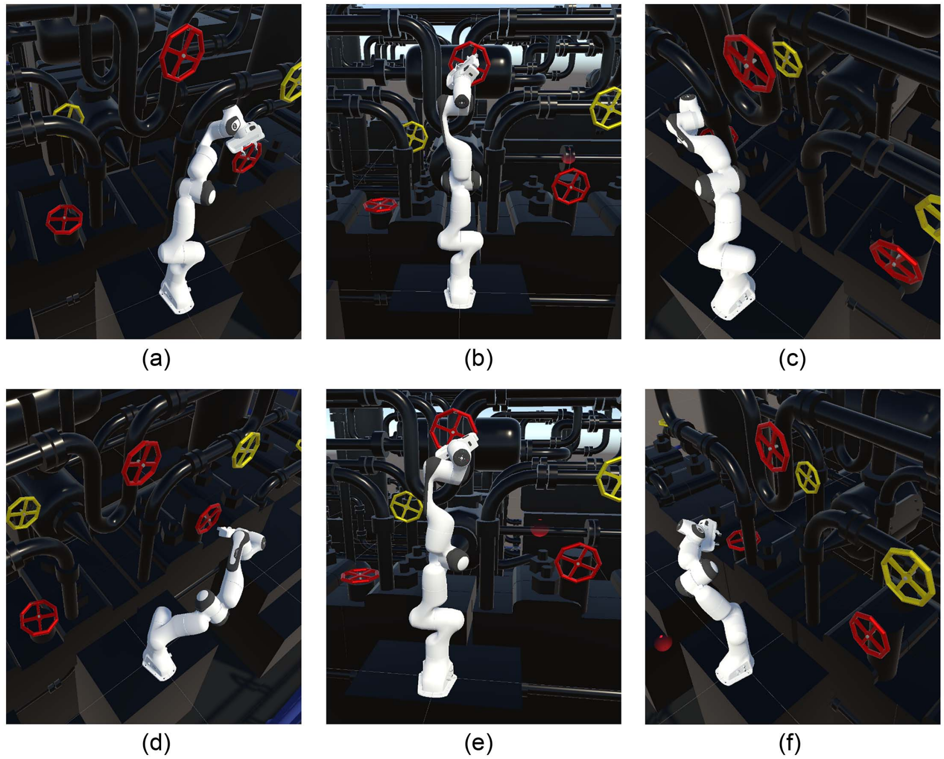


**Fig. 5.** Pipe skid maintenance task with (a–c) humanlike IK; and (d–f) only one IK solver.

participants' learning curve and environmental knowledge on the experimental results, we shuffled the order of the control algorithms in Session 2 and Session 4. The experimental procedure took approximately 30 min for each participant.

During the experiment, human operators were required to wear a VR headset, a VR tracker, and a VR controller to control the robot and interact with the virtual environment. When the robot was activated, the operator can control the end effector through the VR controller to operate each valve.

We recruited a total of 26 subjects for this experiment (12 females, average age of 27). All participants reported that they were right-handed and did not have any known motor disorders or a history of neurological abnormalities. The study was approved by the ethical approval of the ethics committee at the University of Florida. All subjects were required to give their written informed consent before attending the experiment.

### Task Performance Analysis

To capture human operator performance differences under the proposed humanlike IK method and the traditional IK method in construction robot teleoperation, we used both task completion time and collision as evaluation metrics. We tracked performance data from each trial of all subjects and performed a repeated-measure (rm) ANOVA across two conditions. The horizontal line in the box plots represents the median of the data.

The absolute time spent on the valve manipulation task of each trial was counted as the task completion time. As shown in Fig. 6, the results indicate that there is no significant difference ($P = 0.908$ and $F = 0.013$) between the humanlike IK condition and the traditional IK condition in completion time.

In terms of operational accuracy, we measured the total amount of the collision that happened under each trail as collision performance. Fig. 7 compares collisions between the humanlike IK condition and traditional IK condition. The points indicate the collision positions for different conditions. We found that the humanlike IK outperformed the traditional IK with significantly low collision numbers ($P = 0.0001$ and $F = 20.673$). Although there was no significant difference between the humanlike IK condition and traditional IK condition in task completion time, the operational accuracy was dramatically increased based on the humanlike IK control method; the average collision was reduced from 3.865 per trial (traditional IK) to 1.3 per trial (humanlike IK). However, the median values shown as horizontal lines in the box plots showed the opposite.

We also found out that the collisions in traditional IK condition were significantly higher than that of the humanlike IK condition when the $y$-axis was below 0.1. The points below 0.1 on the $y$-axis were the collision between the robot and the bottom plate of the pipe skid. It is possible that in the operation of controlling the robot to move from the left valve to the right valve, the operator could not control the other joints of the robot effectively using the traditional control method. With the humanlike control method, the operator could control other joints more effectively. We also compared the number of collisions only beyond 0.1 on the $y$-axis. The average number of collisions for the traditional IK was 3.587 per trial, which remains significantly higher than the number of collisions of the humanlike IK (1.3 per trial).

### Regularity of Control Velocity

To quantify the controlling speed changes, in terms of velocity regularity during teleoperation, entropy was widely used in previous studies (Pincus and Viscarello 1992). Higher entropy values usually estimate more chaos or irregularity in signals. The Sample Entropy (SampEn Index) (Richman and Moorman 2000) was used in this study because the SampEn index is a predominant metric for human motion or gesture studies to access velocity regularity. In addition, the SampEn method has been shown to have a low bias because its parameter is independent of the length of the records

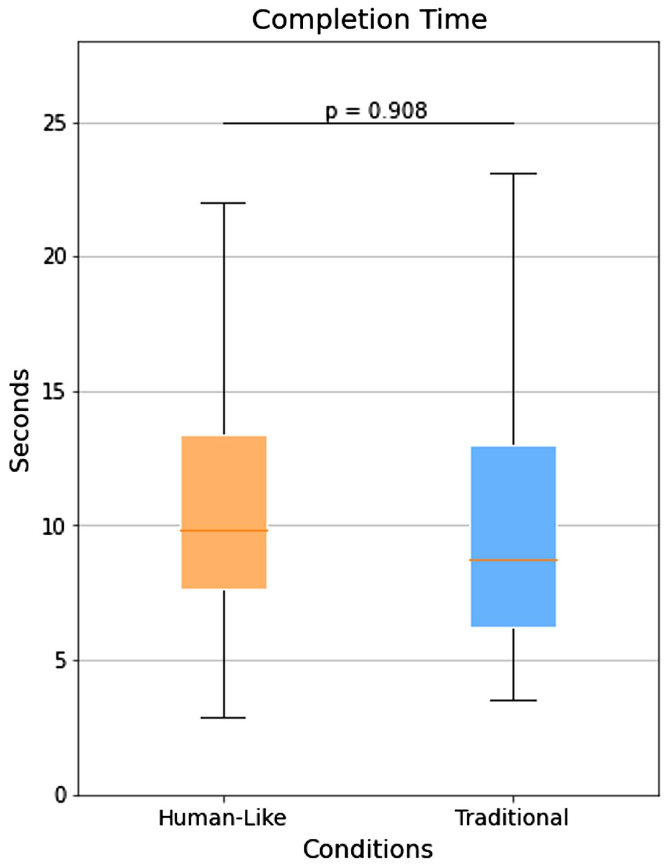


**Fig. 6.** Repeated-measure ANOVA of completion time across the humanlike condition and the traditional condition.

(Yentes et al. 2013). We recorded the control velocity data in all directions $(X, Y, Z)$ of each trial and performed the Sample Entropy calculation.

Based on the frequency of VR data collection, we calculated the velocity according to the position change of each frame

$$V_t = \frac{P_t - P_{t-1}}{T_t - T_{t-1}} \tag{3}$$

We could calculate the velocity for meters per second or meters per frame because 1 frame $= 1/90$ s. The velocity of hand movement, elbow movement, and movement of each robot joint was also calculated.

For a given embedding dimension $m$, tolerance $r$, and the number of data points $N$, SampEn is the negative natural logarithm of the probability that if two sets of simultaneous data points of length $m$ have distance $<r$, then two sets of simultaneous data points of length $m+1$ also have distance $<r$. Assume there is a time-series data set of length $\boldsymbol{N} = \{x_1, x_2, x_3, \ldots, x_N\}$ with a constant time interval $\tau$. The template vector of length is defined as $\boldsymbol{m}$, such that $\boldsymbol{X_m(i)} = \{x_i, x_{i+1}, x_{i+2}, \ldots, x_{i+m-1}\}$ and the distance function $d[\boldsymbol{X_m(i)}, \boldsymbol{X_m(j)}](i \neq j)$ is to be the Chebyshev distance (Cantrell 2000). The sample entropy can be defined as follows:

$$\text{SampEn} = -\ln\frac{A}{B} \tag{4}$$

where

$$A = \text{number of template vector pairs having } d\,[X_{m+1}(i), X_{m+1}(j)] < r \tag{5}$$

$$B = \text{number of template vector pairs having } d\,[X_m(i), X_m(j)] < r \tag{6}$$

The results of the velocity regularity comparison are given in Fig. 8. We observed a significant difference in sample entropy of control velocity in all of the $X$-direction ($P = 0.0048$), $Y$-direction ($P = 0.0189$), and $Z$-direction ($P < 0.0001$) between the humanlike IK and traditional IK conditions. The results show that subjects with humanlike IK control methods tended to have lower sample entropy of controlling velocity, which indicates that they had more constant controlling speed or regular patterns. This may be due to the fact that individuals with a higher level of embodied cognition were more confident in their ability to perform motion coordination tasks and, as a result, exhibited smoother movement.

### Human Operator Subjective Assessments

In addition to task performance, we also analyzed human operators' reported feelings toward task workload, situational awareness, and

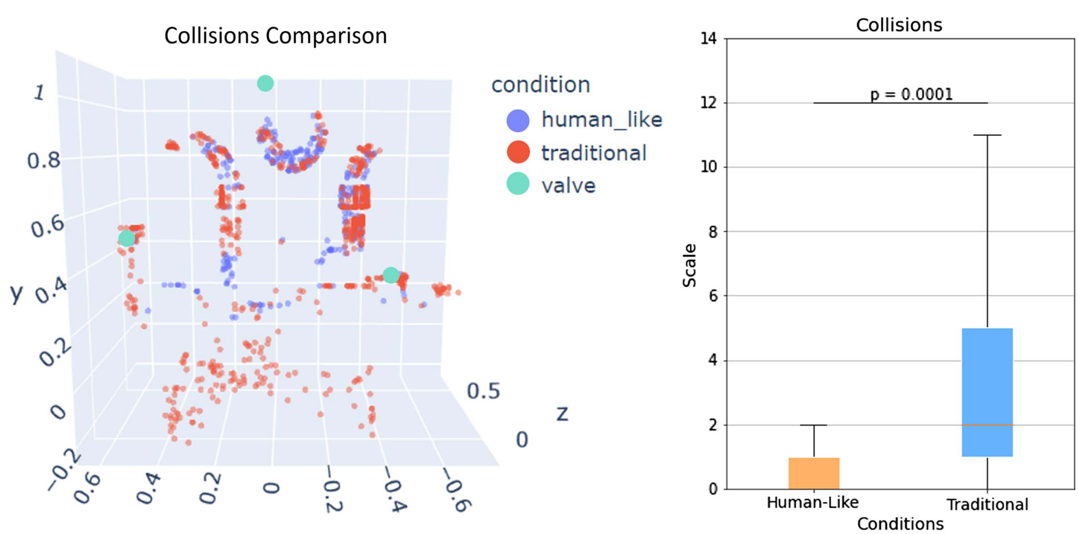


**Fig. 7.** Collision point in 3D view and repeated-measure ANOVA of collision times across the humanlike condition and traditional condition.

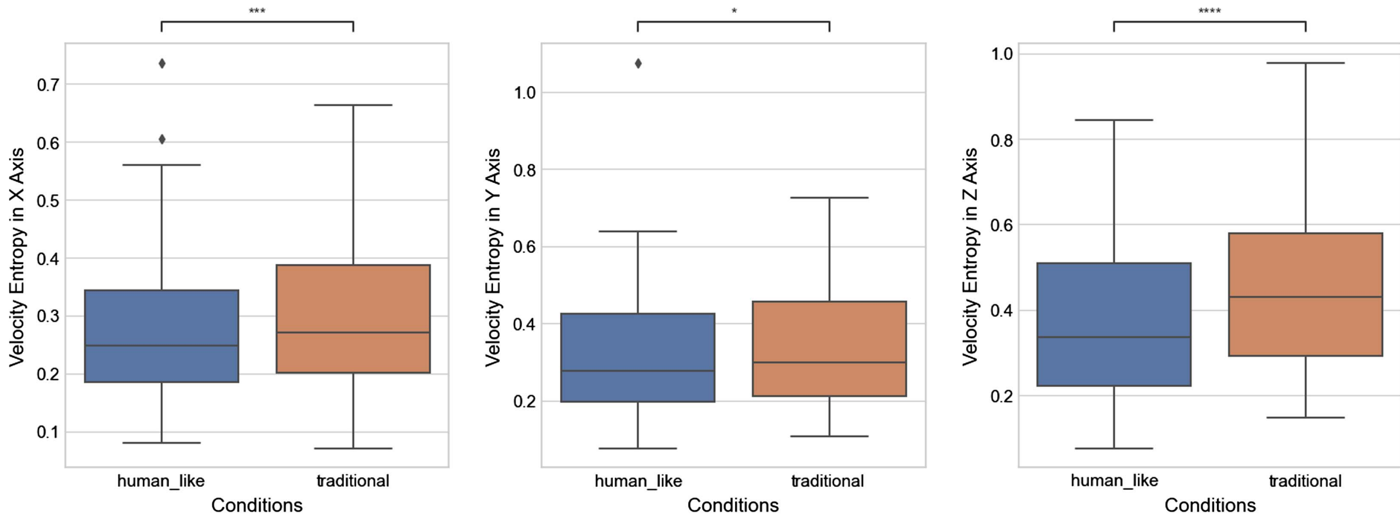


**Fig. 8.** Repeated-measure ANOVA of velocity entropy across the humanlike condition and traditional condition in $X$-, $Y$-, and $Z$-axes.

trust level of the control methods by different questionnaires. Three surveys were taken when the subject finished 10 task trials of each condition. In this way, they could report an overall evaluation of all trials related to the corresponding control method. A rm ANOVA was performed to test whether there were any significant differences between the humanlike IK condition and traditional IK condition in terms of operator subjective assessments.

Six subscale NASA TLX questionnaires (Hart and Staveland 1988) were used to evaluate the workload levels from different perspectives. The subject's reported task workload was calculated as the sum of all six subscales. The results (Fig. 9) revealed that there is no significant difference ($P = 0.316$ and $F = 1.043$) between the humanlike IK condition and traditional IK condition. Similarly, we did not observe biases ($P = 0.731$ and $F = 0.121$) in reported situational awareness levels, which were accessed by the SART survey (Taylor 2017). To capture the human operator's tendency to trust the system and to contextual trust in automation (TiA) behaviors (Kohn et al. 2021), we used a six-item Trust Scale questionnaire (Merritt 2011) to measure the subject's trust levels corresponding to each IK control method. Compared with the traditional IK condition (mean = 32.769), subjects with the humanlike IK method reported significantly ($P = 0.013$ and $F = 7.072$) higher trust scores (mean = 40.769). Even though the proposed humanlike IK did not improve the operator's perception of the remote environment nor reduce the workload during the operation, it did improve the operator's confidence in the robotic system.

## Discussion

The results of the human-subject experiments showed that the proposed humanlike IK method could significantly improve robot teleoperation task performance and human functions. The performance data indicated that there is no significant difference between the humanlike IK condition and the Traditional IK condition in completion time. However, there seemed to be much fewer incidents

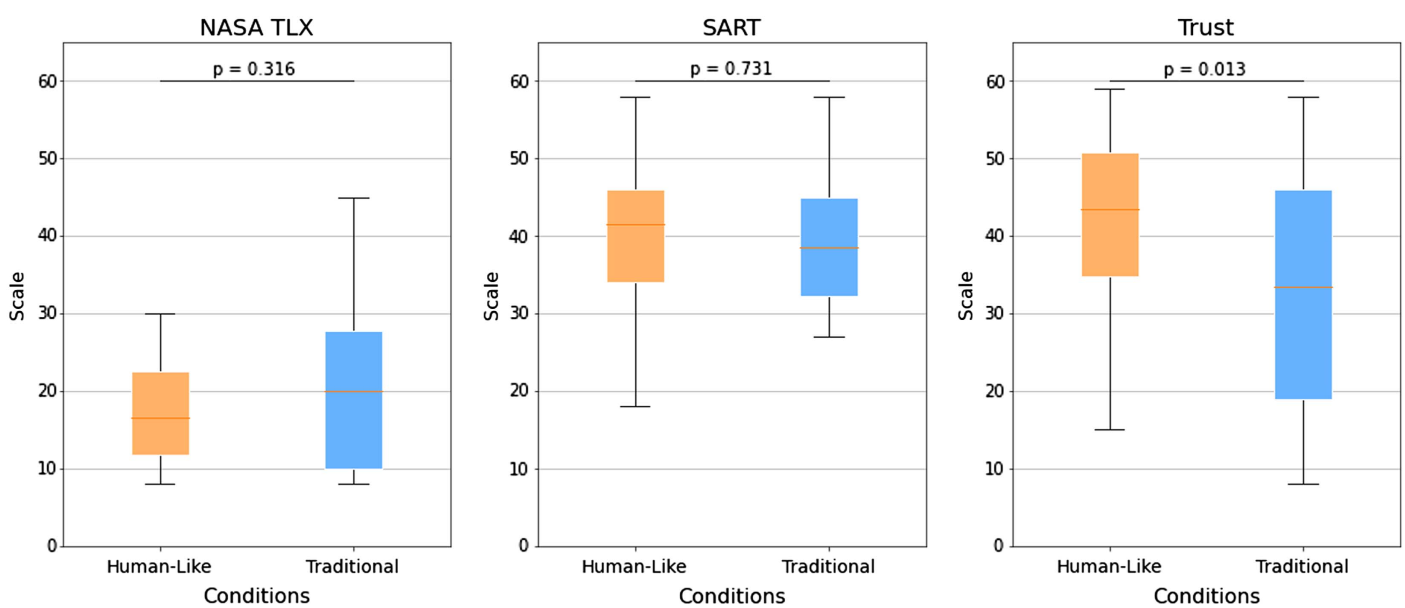


**Fig. 9.** Repeated-measure ANOVA of NASA TLX, SART, and Trust questionnaire across the humanlike condition and traditional condition.

of collisions with the humanlike IK method [66.37% fewer ($P <$ 0.0001)]. Humanlike conditions had fewer collisions when using the same time, which could be attributed to the better embodied cognition induced by the humanlike IK.

Embodied cognition refers to the cognitive process and physical interactions of the human body with the world (Barsalou 1999; Wilson 2002). It is the process whereby which a person uses their sensory structures to create multisensory representations of the surrounding environment and mentally reconstruct an object or action (Barsalou 2003, 2008). Because the humanlike IK may have facilitated faster modeling of a person's own arm in mental representation, especially with the first-person view created by the VR environment, the sensorimotor process may be more effective. It explains why there were fewer incidents of collisions because humans are good at avoiding collisions of their own body parts with obstacles.

The trajectory analysis found that with the humanlike IK method, the entropy of robot end-effector velocity was lower, or more stable [10.21% lower than that of the traditional IK method ($P = 0.0048$) in the $x$-axis, 3.46% lower than that of the traditional IK method ($P = 0.0189$) in the $y$-axis, and 18.79% lower than that of the traditional IK method ($P < 0.0001$) in the $z$-axis]. This could be because with a better embodied cognition, participants were more confident with the motion coordination tasks and hence demonstrated a smoother movement. However, with the traditional IK method, because of the insufficient sense of ownership of the body extension (i.e., the robotic arm as a surrogate of their own arms), the spatial awareness may have been impaired. As a result, participants had to slow down at critical decision points, such as approaching a narrow gap for the far-reaching task. The instantaneous speed changed substantially during the entire task. It was finally shown as a higher entropy.

Subjective perception assessments also confirmed various benefits of the proposed humanlike IK method. There was no significant difference between the humanlike condition and the traditional condition in NASA TLX and SART. For the humanlike condition, the human operators were able to control two poses of the robot, allowing them to spend more effort controlling the robot to the optimal pose to avoid collisions. For the traditional condition, human operators could only control the end effector of the robot. When all the attention was focused on the end effector, it was easier to make a decision. The results of the questionnaire indicated that the participants who exerted greater effort in the humanlike condition did not experience a significant increase in cognitive load, but also improved the experimental outcomes (fewer collisions). A possible explanation for the no significant difference in the situational awareness questionnaire is that the scenario and task for the experiment were simple enough to comprehend. All participants were capable of handling all variables and had excellent situational awareness of both the robot's pose and mission targets. Finally, the use of the humanlike IK method also improved the level of technology trust [24.41% better ($P = 0.013$)]. All of these findings echoed our observation about performance improvement.

## Conclusions

Robot teleoperation has been widely used in various industrial workplaces where the environment is inaccessible or hazardous for human workers. Compared with fully autonomous robotic applications, robot teleoperation combines the abilities of uncertain decision making of human workers and the physical capabilities of robotic systems in dynamic motor tasks. A key challenge for designing an effective teleoperation system is an intuitive control mechanism that enables human operators to control the locomotion of the robot in accordance with the instructed trajectory or the bilateral control. The traditional bilateral control system uses a single-solver IK method to recover the dynamics (i.e., positional changes and rotation) of each joint based on the dynamics of the end effector, which may cause the robotic arm to move in a way undesired by the human operator, leading the robot arm to collide with surrounding objects.

In this study, we proposed and tested an intuitive robot teleoperation IK method that controls the majority of robot arm joints based on inputs from multiple joints of the human arm, called the humanlike IK method. In recognition of the importance of the human elbow joint for upper-limb motions, the humanlike IK divides the robot arm into two segments, marked by a middle joint analogous to a human elbow. Then, it tracks human arm motions based on motion trackers attached to the key arm joints and uses a multivariate IK solver to recover the rotation of each robot joint, especially the pose and position of the robot arm elbow. A human-subject experiment showed that the proposed humanlike IK helps human operators control the robot arm to move in a more natural way similar to the manner of a human arm, reducing the risks of collision and improving both performance and perceptions.

One of the limitations of this research is that we performed the test in a pure simulation environment. This was due to the safety consideration of using a real robot. Collisions with a real robot may damage the robotic system and the structure we used. To demonstrate the similarity between the simulated robotic system and the real robot, we presented a pilot study. It confirmed that simulation and real robotic systems were similar enough because they were both controlled by ROS. But we could not confirm if a simulated environment would trigger similar human behaviors. As a result, one of our future agendas is to perform a system test with a real robotic system in a safe way. Another activity we plan to pursue is to test the differences among different forms of robotic arms. In this test, we chose a 7-DOF robotic arm because of its representativeness in modern industrial applications. The use of more or fewer DOF may cause different designs of the humanlike IK. Lastly, we will also test the proposed method in more tasks with varying contexts and spatial configurations.

## Appendix. Details of Newton-Raphson IK Method

The Appendix illustrates the Newton-Raphson IK method used in this study. The function vector for the Newton-Raphson IK method is

$$\{G(\Theta)\} = \{g_1(\Theta), g_2(\Theta), g_3(\Theta), g_4(\Theta), g_5(\Theta), g_6(\Theta)\}^T \quad (7)$$

where $g_1(\mathbf{\Theta})$, $g_2(\mathbf{\Theta})$, and $g_3(\mathbf{\Theta})$ = translation functions based on the position of the end effector; and $g_4(\mathbf{\Theta})$, $g_5(\mathbf{\Theta})$, and $g_6(\mathbf{\Theta})$ = rotation functions based on the angles of the end effector. The angle vector is

$$\{\Theta\} = \{\theta_1, \theta_2, \theta_3, \theta_4, \theta_5, \theta_6, \theta_7\}^T \quad (8)$$

The following is the form of the given functions to solve:

$$\{G(\Theta)\} = \{0\} \quad (9)$$

Let $[J] = [J(\mathbf{\Theta})]$ as the Newton-Raphson Jacobian Matrix. Make an initial guess to the solution $\{\mathbf{\Theta}_0\}$ and solve

$$[J]\{\delta\Theta_k\} = -\{G(\{\Theta_k\})\} \quad (10)$$

where $k$ = iteration counter. Update the current best guess for the solution $\{\Theta_{k+1}\} = \{\Theta_k\} + \{\delta\Theta_0\}$ until $\|\{\delta\Theta_k\}\| < \varepsilon$.

## Data Availability Statement

All data are available upon request. The video link of the real and virtual robots being controlled in the same pose can be found at https://youtu.be/d6ainvm6sk0. The raw data collected by the system on participants' hand movement, elbow movement, robot joint movement, task complete states, and collision times at a frequency of 90 Hz can be found at https://www.dropbox.com/sh/jbokwdr06wbwecb/AABIdESNJ5WzRodvKl0Zut4ra?dl=0.

## Acknowledgments

This material is supported by the National Science Foundation (NSF) under Grant Nos. 1937053 and 2024784. Any opinions, findings, conclusions, or recommendations expressed in this article are those of the authors and do not reflect the views of the NSF.

## References

Anderson, R. J., and M. W. Spong. 1988. "Bilateral control of teleoperators with time delay." In *Proc., 1988 IEEE Int. Conf. on Systems, Man, and Cybernetics*, 131–138. New York: IEEE.

Aristidou, A., J. Lasenby, Y. Chrysanthou, and A. Shamir. 2018. "Inverse kinematics techniques in computer graphics: A survey." In *Proc., Computer Graphics Forum*, 35–58. New York: Wiley.

Barsalou, L. 2003. "Situated simulation in the human conceptual system." *Lang. Cognit. Processes* 18 (5–6): 513–562. https://doi.org/10.1080/01690960344000026.

Barsalou, L. W. 1999. "Perceptual symbol systems." *Behav. Brain Sci.* 22 (4): 577–660. https://doi.org/10.1017/S0140525X99002149.

Barsalou, L. W. 2008. "Grounded cognition." *Annu. Rev. Psychol.* 59 (5): 617–645. https://doi.org/10.1146/annurev.psych.59.103006.093639.

Bennett, D., J. Hollerbach, Y. Xu, and I. Hunter. 1992. "Time-varying stiffness of human elbow joint during cyclic voluntary movement." *Exp. Brain Res.* 88 (2): 433–442. https://doi.org/10.1007/BF02259118.

Bonci, A., P. D. Cen Cheng, M. Indri, G. Nabissi, and F. Sibona. 2021. "Human-robot perception in industrial environments: A survey." *Sensors* 21 (5): 1571. https://doi.org/10.3390/s21051571.

Buckley, M., A. Yardley, G. Johnson, and D. Cams. 1996. "Dynamics of the upper limb during performance of the tasks of everyday living—A review of the current knowledge base." *Proc. Inst. Mech. Eng., Part H: J. Eng. Med.* 210 (4): 241–247. https://doi.org/10.1243/PIME_PROC_1996_210_420_02.

Buss, S. R. 2004. "Introduction to inverse kinematics with Jacobian transpose, pseudoinverse and damped least squares methods." *IEEE J. Rob. Autom.* 17 (1–19): 16.

Cantrell, C. D. 2000. *Modern mathematical methods for physicists and engineers*. Cambridge, UK: Cambridge University Press.

Canutescu, A. A., and R. L. Dunbrack Jr. 2003. "Cyclic coordinate descent: A robotics algorithm for protein loop closure." *Protein Sci.* 12 (5): 963–972. https://doi.org/10.1110/ps.0242703.

Casalino, A., C. Messeri, M. Pozzi, A. M. Zanchettin, P. Rocco, and D. Prattichizzo. 2018. "Operator awareness in human–Robot collaboration through wearable vibrotactile feedback." *IEEE Rob. Autom. Lett.* 3 (4): 4289–4296. https://doi.org/10.1109/LRA.2018.2865034.

Cavallin, K., and P. Svensson. 2009. *Semi-Autonomous, teleoperated search and rescue robot*. Uppsala, Sweden: Uppsala Univ.

Chen, J. Y., E. C. Haas, and M. J. Barnes. 2007. "Human performance issues and user interface design for teleoperated robots." *IEEE Trans. Syst. Man Cybern. Part C Appl. Rev.* 37 (6): 1231–1245. https://doi.org/10.1109/TSMCC.2007.905819.

Chitta, S. 2016. "Moveit: An introduction." In *Robot operating system (ROS)*, 3–27. Berlin: Springer.

Chitta, S., I. Sucan, and S. Cousins. 2012. "Moveit [ROS topics]." *IEEE Rob. Autom. Mag.* 19 (1): 18–19. https://doi.org/10.1109/MRA.2011.2181749.

Craig, J. J. 2009. *Introduction to robotics: Mechanics and control, 3/E*. Noida, India: Pearson Education.

Crick, C., G. Jay, S. Osentoski, B. Pitzer, and O. C. Jenkins. 2017. "Rosbridge: ROS for non-ROS users." In *Robotics research*, 493–504. Berlin: Springer.

Diankov, R. 2010. "Ikfast: The robot kinematics compiler." Accessed May 23, 2022. http://openrave.org/docs/latest_stable/openravepy/ikfast/#ikfast-the-robot-kinematics-compiler.

Doisy, G., A. Ronen, and Y. Edan. 2017. "Comparison of three different techniques for camera and motion control of a teleoperated robot." *Appl. Ergon.* 58 (5): 527–534. https://doi.org/10.1016/j.apergo.2016.05.001.

Drury, J. L., J. Scholtz, and H. A. Yanco. 2003. "Awareness in human-robot interactions." In *Proc., SMC'03 Conf. Proc. 2003 IEEE Int. Conf. on Systems, Man and Cybernetics. Conf. Theme-System Security and Assurance (Cat. No. 03CH37483)*, 912–918. New York: IEEE.

Du, J., Y. Shi, C. Mei, J. Quarles, and W. Yan. 2016. "Communication by interaction: A multiplayer VR environment for building walkthroughs." In *Proc., Construction Research Congress 2016*, 2281–2290. Reston, VA: ASCE.

Du, J., Y. Shi, Z. Zou, and D. Zhao. 2018a. "CoVR: Cloud-based multiuser virtual reality headset system for project communication of remote users." *J. Constr. Eng. Manage.* 144 (2): 04017109. https://doi.org/10.1061/(ASCE)CO.1943-7862.0001426.

Du, J., Z. Zou, Y. Shi, and D. Zhao. 2017. "Simultaneous data exchange between BIM and VR for collaborative decision making." *Comput. Civ. Eng.* 2017 (Jun): 1–8.

Du, J., Z. Zou, Y. Shi, and D. Zhao. 2018b. "Zero latency: Real-time synchronization of BIM data in virtual reality for collaborative decision-making." *Autom. Constr.* 85 (Jan): 51–64. https://doi.org/10.1016/j.autcon.2017.10.009.

El-Sherbiny, A., M. A. Elhosseini, and A. Y. Haikal. 2018. "A comparative study of soft computing methods to solve inverse kinematics problem." *Ain Shams Eng. J.* 9 (4): 2535–2548. https://doi.org/10.1016/j.asej.2017.08.001.

Emika, F. 2022. "Franka control interface documentation–Franka Control Interface (FCI) documentation." Accessed May 23, 2022. https://frankaemika.github.io/docs/.

Freina, L., and M. Ott. 2015. "A literature review on immersive virtual reality in education: State of the art and perspectives." In *Proc., Int. Scientific Conf. Elearning and Software for Education*, 1101. Bucharest, Romania: Romanian Advanced Distributed Learning Association.

Gan, J. Q., E. Oyama, E. M. Rosales, and H. Hu. 2005. "A complete analytical solution to the inverse kinematics of the Pioneer 2 robotic arm." *Robotica* 23 (1): 123–129. https://doi.org/10.1017/S0263574704000529.

GitHub. 2019. "ROS# GitHub page." Accessed February 6, 2020. https://github.com/siemens/ros-sharp.

Hart, S. G., and L. E. Staveland. 1988. "Development of NASA-TLX (Task Load Index): Results of empirical and theoretical research." In *Advances in psychology*, 139–183. Amsterdam, Netherlands: Elsevier.

Hirche, S., and M. Buss. 2012. "Human-oriented control for haptic teleoperation." *Proc. IEEE* 100 (3): 623–647.

Hitz, G., A. Gotovos, M.-É. Garneau, C. Pradalier, A. Krause, and R. Y. Siegwart. 2014. "Fully autonomous focused exploration for robotic environmental monitoring." In *Proc., 2014 IEEE Int. Conf. on Robotics and Automation (ICRA)*, 2658–2664. New York: IEEE.

Ikuta, K., K. Yamamoto, and K. Sasaki. 2003. "Development of remote microsurgery robot and new surgical procedure for deep and narrow space." In *Proc., 2003 IEEE Int. Conf. on Robotics and Automation (Cat. No. 03CH37422)*, 1103–1108. New York: IEEE.

Ishida, R., L. Meli, Y. Tanaka, K. Minamizawa, and D. Prattichizzo. 2018. "Sensory-motor augmentation of the robot with shared human perception." In *Proc., 2018 IEEE/RSJ Int. Conf. on Intelligent Robots and Systems (IROS)*, New York: IEEE.

Jiang, H., J. P. Wachs, M. Pendergast, and B. S. Duerstock. 2013. "3D joystick for robotic arm control by individuals with high level spinal cord injuries." In *Proc., 2013 IEEE 13th Int. Conf. on Rehabilitation Robotics (ICORR)*, 1–5. New York: IEEE.

Kanehiro, F., H. Hirukawa, K. Kaneko, S. Kajita, K. Fujiwara, K. Harada, and K. Yokoi. 2004. "Locomotion planning of humanoid robots to pass through narrow spaces." In *Proc., IEEE Int. Conf. on Robotics and Automation, 2004*, 604–609. New York: IEEE.

Kenwright, B. 2012. "Inverse kinematics–cyclic coordinate descent (CCD)." *J. Graphics Tools* 16 (4): 177–217. https://doi.org/10.1080/2165347X.2013.823362.

Kim, D., M. Liu, S. Lee, and V. R. Kamat. 2019. "Trajectory prediction of mobile construction resources toward pro-active struck-by hazard detection." In *Proc., Int. Symp. on Automation and Robotics in Construction (IAARC)*. Banff, Canada: IAARC.

Kinateder, M., E. Ronchi, D. Nilsson, M. Kobes, M. Müller, P. Pauli, and A. Mühlberger. 2014. "Virtual reality for fire evacuation research." In *Proc., 2014 Federated Conf. on Computer Science and Information Systems*, 313–321. New York: IEEE.

Kohn, S. C., E. J. De Visser, E. Wiese, Y.-C. Lee, and T. H. Shaw. 2021. "Measurement of trust in automation: A narrative review and reference guide." *Front. Psychol.* 12 (Oct): 604977. https://doi.org/10.3389/fpsyg.2021.604977.

Lander, J., and G. Content. 1998. "Making kine more flexible." *Game Developer Mag.* 1 (15–22): 2.

Lenzi, T., N. Vitiello, S. M. M. De Rossi, S. Roccella, F. Vecchi, and M. C. Carrozza. 2011. "NEUROExos: A variable impedance powered elbow exoskeleton." In *Proc., 2011 IEEE Int. Conf. on Robotics and Automation*, 1419–1426. New York: IEEE.

Li, X., S. Liu, Y. Chang, S. Li, Y. Fan, and H. Yu. 2020. "A human joint torque estimation method for elbow exoskeleton control." *Int. J. Humanoid Rob.* 17 (3): 1950039. https://doi.org/10.1142/S0219843619500397.

Luenberger, D. G., and Y. Ye. 1984. *Linear and nonlinear programming*. Berlin: Springer.

Manocha, D., and J. F. Canny. 1994. "Efficient inverse kinematics for general 6R manipulators." *IEEE Trans. Rob. Autom.* 10 (5): 648–657. https://doi.org/10.1109/70.326569.

Mathew, E. B., D. Khanduja, B. Sapra, and B. Bhushan. 2015. "Robotic arm control through human arm movement detection using potentiometers." In *Proc., 2015 Int. Conf. on Recent Developments in Control, Automation and Power Engineering (RDCAPE)*, 298–303. New York: IEEE.

Merritt, S. M. 2011. "Affective processes in human–automation interactions." *Hum. Factors* 53 (4): 356–370. https://doi.org/10.1177/0018720811411912.

Murphy, R. R. 2004. "Human–robot interaction in rescue robotics." *IEEE Trans. Syst. Man Cybern. Part C Appl. Rev.* 34 (2): 138–153. https://doi.org/10.1109/TSMCC.2004.826267.

Niemeyer, G., C. Preusche, S. Stramigioli, and D. Lee. 2016. "Telerobotics." In *Springer handbook of robotics*, 1085–1108. Berlin: Springer.

Opiyo, S., J. Zhou, E. Mwangi, W. Kai, and I. Sunusi. 2021. "A review on teleoperation of mobile ground robots: Architecture and situation awareness." *Int. J. Control Autom. Syst.* 19 (3): 1384–1407. https://doi.org/10.1007/s12555-019-0999-z.

Osawa, H., A. Ema, H. Hattori, N. Akiya, N. Kanzaki, A. Kubo, T. Koyama, and R. Ichise. 2017. "Analysis of robot hotel: Reconstruction of works with robots." In *Proc., 2017 26th IEEE Int. Symp. on Robot and Human Interactive Communication (RO-MAN)*, 219–223. New York: IEEE.

Paul, R. P., and B. Shimano. 1979. "Kinematic control equations for simple manipulators." In *Proc., IEEE Conf. on Decision and Control including the 17th Symp. on Adaptive Processes*, 1398–1406. New York: IEEE.

Penrose, R. 1955. "A generalized inverse for matrices." In *Proc., Mathematical Cambridge Philosophical Society*, 406–413. Cambridge, UK: Cambridge University Press.

Peternel, L., N. Tsagarakis, and A. Ajoudani. 2017. "A human–robot co-manipulation approach based on human sensorimotor information." *IEEE Trans. Neural Syst. Rehabil. Eng.* 25 (7): 811–822. https://doi.org/10.1109/TNSRE.2017.2694553.

Pincus, S. M., and R. R. Viscarello. 1992. "Approximate entropy: A regularity measure for fetal heart rate analysis." *Obstet. Gynecol.* 79 (2): 249–255.

Pu, G., P. Wei, A. Aribe, J. Boultinghouse, N. Dinh, F. Xu, and J. Du. 2021. "Seeing through walls: Real-time digital twin modeling of indoor spaces." In *Proc., 2021 Winter Simulation Conf. (WSC)*, 1–10. New York: IEEE.

Qian, K., A. Song, J. Bao, and H. Zhang. 2012. "Small teleoperated robot for nuclear radiation and chemical leak detection." *Int. J. Adv. Rob. Syst.* 9 (3): 70. https://doi.org/10.5772/50720.

Qin, Z., P. Wang, J. Sun, J. Lu, and H. Qiao. 2016. "Precise robotic assembly for large-scale objects based on automatic guidance and alignment." *IEEE Trans. Instrum. Meas.* 65 (6): 1398–1411. https://doi.org/10.1109/TIM.2016.2526738.

Quigley, M., K. Conley, B. Gerkey, J. Faust, T. Foote, J. Leibs, R. Wheeler, and A. Y. Ng. 2009. "ROS: An open-source robot operating system." In *Proc., ICRA workshop on open source software*. . New York: IEEE.

Raghavan, M., and B. Roth. 1993. *Inverse kinematics of the general 6R manipulator and related linkages*. New York: ASME.

Rakita, D., B. Mutlu, and M. Gleicher. 2018. "An autonomous dynamic camera method for effective remote teleoperation." In *Proc., 2018 ACM/IEEE Int. Conf. on Human-Robot Interaction*, 325–333. New York: IEEE.

Reddivari, H., C. Yang, Z. Ju, P. Liang, Z. Li, and B. Xu. 2014. "Teleoperation control of Baxter robot using body motion tracking." In *Proc., 2014 Int. Conf. on Multisensor Fusion and Information Integration for Intelligent systems (MFI)*, 1–6. New York: IEEE.

Richman, J. S., and J. R. Moorman. 2000. "Physiological time-series analysis using approximate entropy and sample entropy." *Am. J. Physiol. Heart Circle Physiol.* 2000 (Jun): 2039–2049. https://doi.org/10.1152/ajpheart.2000.278.6.H2039.

Scholtz, J. 2003. "Theory and evaluation of human robot interactions." In *Proc., 36th Annual Hawaii Int. Conf. on System Sciences*. New York: IEEE.

Sciavicco, L., and B. Siciliano. 2012. *Modelling and control of robot manipulators*. Berlin: Springer.

Sheridan, T. B. 1992. *Telerobotics, automation, and human supervisory control*. Cambridge, MA: MIT Press.

Shi, Y., J. Du, E. Ragan, K. Choi, and S. Ma. 2018. "Social influence on construction safety behaviors: A multi-user virtual reality experiment." In *Proc., Construction Research Congress*, 147–183. Reston, VA: ASCE.

Shou, W., J. Wang, and X. Wang. 2018. "4D BIM for improving plant turnaround maintenance planning and execution: A case study." In *Proc., ISARC. Int. Conf. Symp. on Automation and Robotics in Construction*, 1–8. Waterloo, ON: IAARC Publications.

Shukla, A., and H. Karki. 2016. "Application of robotics in offshore oil and gas industry—A review Part II." *Rob. Auton. Syst.* 75 (Jun): 508–524. https://doi.org/10.1016/j.robot.2015.09.013.

Siciliano, B., and O. Khatib. 2016. *Springer handbook of robotics*. Berlin: Springer.

Siemens. 2019. "Siemens/ROS-sharp." Accessed February 6, 2020. https://github.com/siemens/ros-sharp.

Stanton, C., A. Bogdanovych, and E. Ratanasena. 2012. "Teleoperation of a humanoid robot using full-body motion capture, example movements, and machine learning." In *Proc., Australasian Conf. on Robotics and Automation*, 51. Melbourne, VIC, Australia: Australian Robotics and Automation Association.

Taylor, R. M. 2017. "Situational awareness rating technique (SART): The development of a tool for aircrew systems design." In *Situational awareness*, 111–128. Abingdon, UK: Routledge.

Thirumurugan, J., M. Vinoth, G. Kartheeswaran, and M. Vishwanathan. 2010. "Line following robot for library inventory management system." In *Proc., INTERACT-2010*, 1–3. New York: IEEE.

van Osch, M., D. Bera, K. van Hee, Y. Koks, and H. Zeegers. 2014. "Tele-operated service robots: ROSE." *Autom. Constr.* 39 (6): 152–160. https://doi.org/10.1016/j.autcon.2013.06.009.

Vu, M. T., H.-S. Choi, N. D. Nguyen, and S.-K. Kim. 2019. "Analytical design of an underwater construction robot on the slope with an up-cutting mode operation of a cutter bar." *Appl. Ocean Res.* 86 (Jun): 289–309. https://doi.org/10.1016/j.apor.2019.02.019.

Wang, L.-C., and C.-C. Chen. 1991. "A combined optimization method for solving the inverse kinematics problems of mechanical manipulators." *IEEE Trans. Rob. Autom.* 7 (4): 489–499. https://doi.org/10.1109/70.86079.

Welman, C. 1993. "Inverse kinematics and geometric constraints for articulated figure manipulation." Ph.D. thesis, School of Computing Science, Simon Fraser Univ.

Wiki, R. 2019. "URDF." Accessed February 6, 2020. http://wiki.ros.org/urdf.

Wilson, M. 2002. "Six views of embodied cognition." *Psychonomic Bull. Rev.* 9 (4): 625–636. https://doi.org/10.3758/BF03196322.

Xia, P., F. Xu, Q. Zhu, and J. Du. 2022. "Human robot comparison in rapid structural inspection." In *Proc., Construction Research Congress 2022*, 570–580. Reston, VA: ASCE.

Yanco, H. A., and J. Drury. 2004. "Classifying human-robot interaction: An updated taxonomy." In *Proc., 2004 IEEE Int. Conf. on Systems, Man and Cybernetics (IEEE Cat. No. 04CH37583)*, 2841–2846. New York: IEEE.

Yanco, H. A., and J. L. Drury. 2002. "A taxonomy for human-robot interaction." In *Proc., AAAI Fall Symp. on Human-Robot Interaction*, 111119. Palo Alto, CA: Association for the Advancement of Artificial Intelligence.

Yang, C., X. Wang, L. Cheng, and H. Ma. 2016. "Neural-learning-based telerobot control with guaranteed performance." *IEEE Trans. Cybern.* 47 (10): 3148–3159. https://doi.org/10.1109/TCYB.2016.2573837.

Yentes, J. M., N. Hunt, K. K. Schmid, J. P. Kaipust, D. McGrath, and N. Stergiou. 2013. "The appropriate use of approximate entropy and sample entropy with short data sets." *Ann. Biomed. Eng.* 41 (2): 349–365. https://doi.org/10.1007/s10439-012-0668-3.

Yokokohji, Y., and T. Yoshikawa. 1994. "Bilateral control of master-slave manipulators for ideal kinesthetic coupling-formulation and experiment." *IEEE Trans. Rob. Autom.* 10 (5): 605–620. https://doi.org/10.1109/70.326566.

Zhou, T., Y. Wang, Q. Zhu, and J. Du. 2022. "Human hand motion prediction based on feature grouping and deep learning: Pipe skid maintenance example." *Autom. Constr.* 138 (Jun): 104232. https://doi.org/10.1016/j.autcon.2022.104232.

Zhou, T., Q. Zhu, and J. Du. 2020. "Intuitive robot teleoperation for civil engineering operations with virtual reality and deep learning scene reconstruction." *Adv. Eng. Inf.* 46 (Oct): 101170. https://doi.org/10.1016/j.aei.2020.101170.

Zhu, Q., J. Du, Y. Shi, and P. Wei. 2021. "Neurobehavioral assessment of force feedback simulation in industrial robotic teleoperation." *Autom. Constr.* 126 (Jun): 103674. https://doi.org/10.1016/j.autcon.2021.103674.

Zhu, Q., T. Zhou, and J. Du. 2022. "Upper-body haptic system for snake robot teleoperation in pipelines." *Adv. Eng. Inf.* 51 (Jan): 101532. https://doi.org/10.1016/j.aei.2022.101532.